1521-0103/12/3402-360–368
THE JOURNAL OF PHARMACOLOGY AND EXPERIMENTAL THERAPEUTICS
U.S. Government work not protected by U.S. copyright
JPET 340:360–368, 2012

Vol. 340, No. 2
187948/3742537

Changes in Mouse Liver Protein Glutathionylation after Acetaminophen Exposure

Xi Yang, James Greenhaw, Akhtar Ali, Qiang Shi, Dean W. Roberts, Jack A. Hinson, Levan Muskhelishvili, Richard Beger, Lisa M. Pence, Yosuke Ando, Jinchun Sun, Kelly Davis, and William F. Salminen

Division of Systems Biology (X.Y., J.G., A.A., Q.S., R.B., L.M.P., Y.A., J.S., W.F.S.) and Toxicologic Pathology Associates (L.M., K.D.), National Center for Toxicological Research, Jefferson, Arkansas; and Departments of Pediatrics (D.W.R.) and Pharmacology and Toxicology (J.A.H.), University of Arkansas for Medical Sciences, Little Rock, Arkansas

Received September 14, 2011; accepted October 31, 2011

ABSTRACT

The role of protein glutathionylation in acetaminophen (APAP)-induced liver injury was investigated in this study. A single oral gavage dose of 150 or 300 mg/kg APAP in B6C3F1 mice produced increased serum alanine aminotransferase and aspartate aminotransferase levels and liver necrosis in a dose-dependent manner. The ratio of GSH to GSSG was decreased in a dose-dependent manner, suggesting that APAP produced a more oxidizing environment within the liver. Despite the increased oxidation state, the level of global protein glutathionylation was decreased at 1 h and continued to decline through 24 h. Immunohistochemical localization of glutathionylated proteins showed a complex dynamic change in the lobule zonation of glutathionylated proteins. At 1 h after APAP exposure, the level of glutathionylation decreased in the single layer of hepatocytes around the central veins but increased mildly in the remaining centrilobular hepatocytes. This increase correlated with the immunohistochemical localization of APAP covalently bound to protein. Thereafter, the level of glutathionylation decreased dramatically over time in the centrilobular regions with major decreases observed at 6 and 24 h. Despite the overall decreased glutathionylation, a layer of cells lying between the undamaged periportal region and the damaged centrilobular hepatocytes exhibited high levels of glutathionylation at 3 and 6 h in all samples and in some 24-h samples that had milder injury. These temporal and zonal pattern changes in protein glutathionylation after APAP exposure indicate that protein glutathionylation may play a role in protein homeostasis during APAP-induced hepatocellular injury.

Introduction

Acetaminophen (APAP; 4′-hydroxyacetanilide) is a widely used over-the-counter analgesic and antipyretic in the United States. When used at the recommended therapeutic doses, APAP is rarely associated with liver injury. Unfortunately, APAP can cause fatal acute liver failure when therapeutic doses are exceeded. This can occur when people purposely take an overdose or accidentally consume multiple products containing APAP. Because of this concern, a Food and Drug Administration Advisory Panel recommended lowering the maximum therapeutic dose of APAP (Food and Drug Administration, 2009), and this was followed by a Federal Register notice lowering the maximum APAP dose in prescription products (Food and Drug Administration, 2011).

Because of the concern over APAP-induced liver injury, a tremendous amount of research has been conducted to understand the mechanisms behind the pathogenesis. The least controversial and most critical step is the metabolism of APAP. At therapeutic doses, APAP is metabolized predominantly by the phase II metabolic pathways of glucuronidation and sulfation. A small portion of APAP is metabolized by the phase I cytochrome P450 metabolic pathway to the reactive

X.Y. was supported by the Research Participation Program at the National Center for Toxicological Research, which is administered by the Oak Ridge Institute for Science and Education through an interagency agreement between the U.S. Department of Energy and the U.S. Food and Drug Administration. D.W.R. was supported, in part, by the National Institutes of Health National Institute of Diabetes and Digestive and Kidney Diseases [Grant DK081406], the Arkansas Children's Hospital Research Institute, and the Arkansas Biosciences Institute, the major research component of the Tobacco Settlement Proceeds Act of 2000. J.A.H. was supported by the National Institutes of Health National Institute of Diabetes and Digestive and Kidney Diseases [Grant R01-DK079008].

D.W.R. and J.A.H. are part owners of Acetaminophen Toxicity Diagnostics, LLC, a company working to develop a medical device for diagnosis of acetaminophen-induced liver injury.

Article, publication date, and citation information can be found at http://jpet.aspetjournals.org.

http://dx.doi.org/10.1124/jpet.111.187948.

ABBREVIATIONS: APAP, acetaminophen; NAPQI, *N*-acetyl-*p*-benzoquinoneimine; ALT, alanine aminotransferase; AST, aspartate aminotransferase; MPT, mitochondrial permeability transition; PBS, phosphate-buffered saline; BSA, bovine serum albumin; PAGE, polyacrylamide gel electrophoresis; RT, room temperature; TTBS, Tris-buffered saline containing 1% Tween 20.

metabolite *N*-acetyl-*p*-benzoquinone imine (NAPQI), which is subsequently detoxified by conjugation with GSH (Bessems and Vermeulen, 2001; Hinson et al., 2010). In overdose situations, the glucuronidation and sulfation pathways are overwhelmed, and a larger portion of APAP is metabolized through the phase I pathway. GSH levels are limited and once depleted below a critical level NAPQI is free to react with cellular macromolecules.

After formation of significant quantities of NAPQI, the subsequent pathways leading to cellular injury have been extensively investigated, but their contributions to the actual pathogenesis are more tentative (Jaeschke, 2005; Hinson et al., 2010). Based on the weight of evidence, APAP binds to various proteins and disrupts their function, leading to altered cellular function. However, there are likely to be other direct or indirect effects of NAPQI leading to cell death, such as alteration of cellular redox status or disruption of signaling pathways. Despite the wide array of cellular pathways that have been shown to play a role in APAP-induced hepatotoxicity, it is clear that disruption of mitochondrial function is one of the key outcomes (Masubuchi et al., 2005; Hanawa et al., 2008; Burke et al., 2010). After covalent binding and GSH depletion occur, APAP induces the mitochondrial permeability transition (MPT), which allows the leakage of mitochondrial constituents into the cytosol. After activation of the MPT, mitochondria swell, lose membrane potential, and exhibit decreased oxidative phosphorylation with subsequent ATP depletion and necrotic cell death.

Although these are the key events that have been elucidated to date, there are probably other unidentified factors that play a role in the molecular pathogenesis. Given the significant GSH depletion that occurs after APAP overdose, it is likely that the dramatically altered redox status plays both direct and indirect roles in the pathogenesis. One such potential effect is a change in protein glutathionylation and subsequent altered protein function. Glutathionylation involves the addition of GSH to free sulfhydryl groups on proteins through a disulfide bond. The process is reversible so glutathionylation can change dynamically with changes in redox status, such as increased glutathionylation noted after hydrogen peroxide or O^2-[2,4-dinitro-5-[4-(*N*-methylamino) benzoyloxy]phenyl]-1-(*N,N*-dimethylamino)diazen-1-ium-1,2-diolate exposure (Townsend, 2007). This study was conducted to assess the affect of APAP, and the subsequent altered redox status, on protein glutathionylation in mouse liver.

Materials and Methods

Chemicals. Unless indicated otherwise, all chemicals were purchased from Sigma-Aldrich (St. Louis, MO). Protein separation equipment and reagents including electrophoresis, precast polyacrylamide gels, premixed buffers, loading buffer, and protein standard were purchased from Bio-Rad Laboratories (Hercules, CA). Nitrocellulose/Filter Paper Sandwich and phosphate-buffered saline (PBS) buffer were purchased from Invitrogen (Carlsbad, CA).

Animals. Six- to 7-week-old male B6C3F1 mice, provided by the Food and Drug Administration's National Center for Toxicological Research breeding colonies, were used for the study. Animal care was performed in accordance with the *Guide for the Care and Use of Laboratory Animals* (Institute of Laboratory Animal Resources, 1996) and was authorized by the National Center for Toxicological Research Institutional Animal Care and Use Committee. After a 7-day acclimation period, mice were assigned to experimental groups by weight averaging and housed individually in polycarbonate cages with hardwood chip bedding. During the study, room temperature (RT) remained within 19 to 23°C, and fluorescent lighting was provided on a 12-h on/off cycle. Filtered tap water was provided ad libitum, and an NIH-41-irradiated diet was provided ad libitum except during designated periods of fasting. Mice were fasted overnight for at least 12 h before a single oral (gavage) dose of APAP (suspended in 0.5% methylcellulose) with feed provided to the animals 4 h after dosing. There were three to four mice in the 0.5% methylcellulose control groups and four to five mice in the APAP low-dose (150 mg/kg) and high-dose (300 mg/kg) groups.

Clinical Pathology/Histopathology. Approximately 1, 3, 6, and 24 h after dosing, the mice were anesthetized with carbon dioxide, blood was withdrawn via cardiac puncture, and the mice were then euthanized by carbon dioxide asphyxiation. Blood was collected into a serum separator or EDTA tubes (BD Biosciences, San Jose, CA). Blood in the serum separator tube was allowed to clot for 30 to 60 min at room temperature and centrifuged at 1000*g* for approximately 10 min, and the serum was analyzed on an automated clinical chemistry analyzer (Alfa Wassermann, West Caldwell, NJ) to assess levels of creatinine, blood urea nitrogen, alanine aminotransferase (ALT), aspartate aminotransferase (AST), alkaline phosphatase, γ-glutamyl transferase, glucose, cholesterol, triglycerides, calcium, phosphorus, albumin, total protein, and total bilirubin. Blood in the EDTA tube was analyzed the same day as collection on an ABX Pentra 60 C+ analyzer (ABX, Irvine, CA) for determination of red and white blood cell counts, hemoglobin, hematocrit, mean corpuscular hemoglobin concentration, mean corpuscular volume, platelets, and differential white blood cell count. A gross necropsy was conducted on all animals and included the examination of all major organs, body cavities, and external surfaces. The brain, heart, kidneys, liver, lung, and testes were weighed. Sections of the liver were fixed in neutral buffered 10% formalin for approximately 48 h and then routinely processed, embedded in paraffin, sectioned at 4 to 5 μm, stained with hematoxylin and eosin, and examined by light microscopy by a board-certified veterinary pathologist. Lesions were scored on a five-point scale (0, normal; 1, minimal; 2, mild; 3, moderate; 4, marked).

GSH/GSSG Analysis. Immediately after euthanasia, the liver was quickly removed from the animal, flash-frozen in an isopentane/dry ice slurry, and then stored at −80°C until analysis. A portion (~50 mg) was homogenized in 500 μl of cold methanol (stored at −20°C). Labeled internal standard $^{13}C_2$,^{15}N-GSH (Cambridge Isotope Laboratories, Inc., Andover, MA) was added to the homogenized sample and centrifuged for 15 min at 13,000*g* and 4°C, then the supernatant was transferred and concentrated by using a Savant SpeedVac Plus SC 110A vacuum concentrator (Thermo Fisher Scientific, Waltham, MA). Dried samples were reconstituted in 500 μl of 5% acetonitrile, vortexed, and then centrifuged for 15 min at 13,000*g* and 4°C. GSH/GSSG was separated on a Waters (Milford, MA) BEH reverse-phase C18 column (2.1 × 100 mm, 1.7-μm particle size) with mobile phase A of 0.1% formic acid in water and mobile phase B of 0.1% formic acid in acetonitrile. Analytes were detected by using a Xevo Triple Quadrupole Mass Spectrometer (Waters) in positive electrospray ionization mode with multiple reaction monitoring transitions: *m/z* 308.16 → 179.08 and *m/z* 308.16 → 162.03 (GSH) with a cone voltage of 18 and collision energies of 12 and 16 V, respectively: *m/z* 613.34 → 355.10 and *m/z* 613.34 → 231.09 (GSSG) with cone voltage of 34 and collision energies of 24 and 38 V, respectively; *m/z* 311.16 > 182.08 ($^{13}C_2$,^{15}N-GSH-labeled GSH) with cone voltage of 12 and collision energy of 14 V. Capillary voltage was 3.5 kV, source temperature was 120°C, desolvation temperature was 350°C, and desolvation gas flow rate was 700 l/h.

Western Blots. The protein S-glutathionylation levels in total liver protein were detected by SDS-PAGE and Western blotting as described previously (Beer et al., 2004) with the following modifications. Fifty milligrams of liver was homogenized in lysis buffer (20

mM Tris-HCL, pH 8, 137 mM NaCl, 10% glycerol, 1% Triton X-100, and 2 mM EDTA) with fresh protease inhibitor cocktail (Sigma-Aldrich) using a FastPrep instrument (MP Biomedicals, Solon, OH). After centrifugation for 15 min at 13,000*g* at 4°C, the supernatant was kept at −80°C until use. Protein concentration was determined by the Bradford method using Bio-Rad Protein Assay reagent and bovine serum albumin (BSA) as a standard. Equal amounts (10 μg) of liver lysates were loaded on a 15-well 12% SDS-polyacrylamide gel; proteins were separated under nonreducing conditions. After electrophoresis, proteins were transferred to nitrocellulose membranes (Invitrogen). On completion, membranes were blocked in Tris-buffered saline containing 1% Tween 20 (TTBS) containing 1% (w/v) BSA for 1 h and then probed with anti-*S*-glutathione IgG2a mouse monoclonal antibody (αGSH; ViroGen Corp., Watertown, MA) at a 1:1000 dilution in TTBS/1% BSA overnight. They were washed three times, 10 min per wash, in TTBS, followed by incubation with alkaline phosphatase-conjugated anti-mouse antibody at 1:10,000 dilution in TTBS/1% BSA for 1 h. After three washes, 15 min per wash, the membranes were visualized by using 5-bromo-4-chloro-3-indolyl phosphate/nitro blue tetrazolium liquid substrate. In a separate nonreducing electrophoresis, gels were stained with Coomassie blue (Bio-Rad Laboratories) to assure equal loading of samples. Western blots and Coomassie-stained gels were visualized by using an Odyssey Infrared Imaging System (LI-COR Biosciences, Lincoln, NE) with default settings. The lanes on each blot were automatically detected, and the overall glutathionylation levels were defined by five rectangular boxes, which covered each complete lane. The intensity value of each sample was the sum of the intensity profiles of the five boxes. The intensity value of each sample was adjusted by the Coomassie staining gel intensity to correct for protein loading variations.

Immunohistochemical Analysis of Liver Protein S-Glutathionylation. From each animal, serial sections 4 to 5 μm thick were cut from the block of paraffin-embedded liver to facilitate comparison of localization of glutathione-protein complexes, APAP-reactive metabolite binding, and morphological changes. One section was stained with hematoxylin and eosin and examined for histopathology by light microscopy, and the remaining sections were immunohistochemically stained with αGSH antibody (the same antibody used for Western blots) or an anti-APAP antibody as follows. For immunohistochemical detection of protein glutathionylation or 3-(cystein-*S*-yl)-acetaminophen protein adduct, deparaffinized tissue sections were placed in an antigen retrieval solution (0.01 M citrate buffer, pH 6.0) for 15 min in a microwave oven at 100°C at 600 W. Endogenous peroxidase was inhibited by incubation with freshly prepared 3% hydrogen peroxide with 0.1% sodium azide for 10 min at RT. Nonspecific staining was blocked with 0.5% casein for 20 min at RT. The sections were incubated with αGSH antibody at a dilution of 1:200 (5.0 μg/ml) or rabbit anti-APAP protein adduct antiserum (Matthews et al., 1997) (1:400) for 1 h at RT. After incubation with primary antibody, tissue sections were incubated with biotinylated goat anti-mouse IgG $F(ab)_2$ fragments (Rockland Immunochemicals, Gilbertsville, PA) or anti-rabbit biotinylated IgG (ExtrAvidin Kit; Sigma-Aldrich) for 30 min at RT and later with streptavidin-conjugated horseradish peroxidase (Sigma-Aldrich) for 30 min at RT. Staining was developed with diaminobenzidine (Sigma-Aldrich) substrate for 5 min at RT, and sections were counterstained with hematoxylin and mounted with Permount (Thermo Fisher Scientific). For the negative control, 5.0 μg/ml mouse IgG (Jackson ImmunoResearch Laboratories Inc., West Grove, PA) or PBS replaced the primary antibodies. PBS containing 1% BSA (Sigma-Aldrich) was used as a diluent for working dilutions of the primary antibodies, biotin-conjugated secondary antibodies, streptavidin-conjugated horseradish peroxidase label, and mouse IgG. Between the steps of the staining procedure, slides were washed in PBS for 5 min at RT. All sections were examined by light microscopy (BX40; Olympus, Tokyo, Japan).

Statistical Analysis. All statistical analyses were performed using SigmaPlot version 11.0 for Windows (Systat Software Inc., San Jose, CA). Data were analyzed by a one-way analysis of variance followed by a Student-Neuman-Keuls post hoc test. The level of significance was defined as the 0.05 level of probability. ALT and AST data were log-transformed before statistical analysis.

Results

Clinical and Histopathological Indices of APAP-Induced Liver Injury. A single oral gavage dose of 150 or 300 mg/kg APAP induced a dose-dependent increase in serum ALT and AST (Table 1). Other clinical chemistry parameters were unaffected by APAP (data not shown). Increased ALT and AST values were observed as early as 1 h after treatment at the higher 300 mg/kg APAP dose; whereas statistically significant increases at 150 mg/kg were not observed until 6 and 24 h after dosing (Table 1). Histopathological changes corroborated with the serum ALT and AST results. Centrilobular hepatocellular degeneration was observed at 1 h after dosing with centrilobular hepatocellular necrosis rimmed by degeneration occurring as early as 3 h after dosing. Hepatocellular necrosis rimmed by degeneration surrounding cen-

TABLE 1

Indices of hepatocellular injury in mice after a single oral dose of APAP

Mice (n = 3–5) were administered a single oral gavage dose of 0.5% methylcellulose vehicle (control) or APAP. Blood and liver were collected at the specified times after dosing. Liver histopathology lesions were scored on a five-point scale (0, normal; 1, minimal; 2, mild; 3, moderate; 4, marked). Histopathology scores were not statistically analyzed. Values are mean ± (S.E.M.).

Group	Time	Serum Activity		Histopathology	
		ALT	AST	Centrilobular Degeneration	Centrilobular Necrosis
	h	*IU/l*			
Control	1	34 ± (4)	94 ± (19)	0	0
	3	62 ± (10)	105 ± (5)	0	0
	6	41 ± (6)	83 ± (10)	0	0
	24	44 ± (6)	78 ± (15)	0	0
150 mg/kg	1	41 ± (5)	101 ± (10)	0.8 ± (0.3)	0
	3	126 ± (26)	173 ± (40)	0.8 ± (0.3)	0.3 ± (0.3)
	6	2945 ± (2446)*	2897 ± (2395)*	1.8 ± (0.6)	1.5 ± (0.6)
	24	4547 ± (1902)*	2935 ± (1508)	1.4 ± (0.4)	2.0 ± (0.5)
300 mg/kg	1	979 ± (619)*	1325 ± (793)*	2.0 ± (0.0)	0
	3	5927 ± (2036)*	7471 ± (2542)*	1.8 ± (0.3)	1.5 ± (0.5)
	6	11,475 ± (3987)*	8430 ± (2140)*	2.8 ± (0.2)	2.8 ± (0.4)
	24	9783 ± (2984)*	7469 ± (2497)*	1.8 ± (0.5)	2.8 ± (0.7)

* Statistically significant increase compared with the control at the same time point ($P < 0.05$).

tral veins and often extending around sublobular/hepatic veins was observed at 6 and 24 h after dosing with some high-dose animals exhibiting marked necrosis at 24 h.

APAP Treatment and the Oxidative State of the Liver. The high dose of APAP (300 mg/kg) induced a profound decrease in hepatic GSH at 1 h with levels starting to increase at 3 h and recovery within 6 h (Fig. 1). These results are consistent with those observed in previous studies (Adams et al., 1983; Smith and Jaeschke, 1989; Chen et al., 1990; Jaeschke, 1990; Srinivasan et al., 2001; Knight et al., 2002; Acharya and Lau-Cam, 2010). The low dose of APAP (150 mg/kg) seemed to maintain a lower level of GSH compared with controls, but the difference was not statistically significant. GSSG was not significantly altered for either treated group at 1 or 3 h; however, by 6 h, GSSG levels were significantly increased in the high-dose group (Fig. 1).

The absolute levels of GSH and GSSG give an indication of the oxidative state of the liver; however, another indicator that better portrays the oxidative balance is the ratio of GSH to GSSG. At 1 h, the low dose had a ratio similar to controls; whereas the high dose had a profound decrease in the GSH/GSSG ratio compared with controls (Fig. 2), suggesting a more oxidative environment. At 3 and 6 h, both the low- and high-dose groups had significantly decreased GSH/GSSG ratios, suggesting that both treatments created a more oxidative environment (Fig. 2).

Decreased Global Hepatic Protein Glutathionylation after APAP Exposure. Hepatic protein glutathionylation levels were measured by nondenaturing SDS-PAGE followed by Western blotting using a monoclonal anti-GSH antibody that recognizes glutathiolynated proteins. Control samples had a wide range of hepatic proteins that were glutathiolynated (Fig. 3A). After APAP dosing, the level of global glutathionylation was slightly decreased compared with controls at the 1- and 3-h time points (data not shown) but dramatically decreased, particularly in some individual samples, at the 6- and 24-h time points (Figs. 3A and 4A). Coomassie staining of separate polyacrylamide gels loaded with the same samples confirmed that protein loading was similar across all samples and the decrease in glutathionylation was not an artifact of protein loading (Fig. 3B). Regression analyses between overall glutathionylation level and histopathology score were conducted for the 6- and 24-h time points. At 6 h, decreased glutathionylation levels correlated with increasing severity of histopathological necrosis (Fig. 4B). A similar trend was noted at 24 h (data not shown). To confirm the specificity of the anti-GSH antibody for reversibly glutathiolynated proteins, liver homogenates were first reduced with dithiothreitol before SDS-PAGE to remove reversibly bound GSH. The reducing treatment essentially eliminated anti-GSH binding in these samples (data not shown).

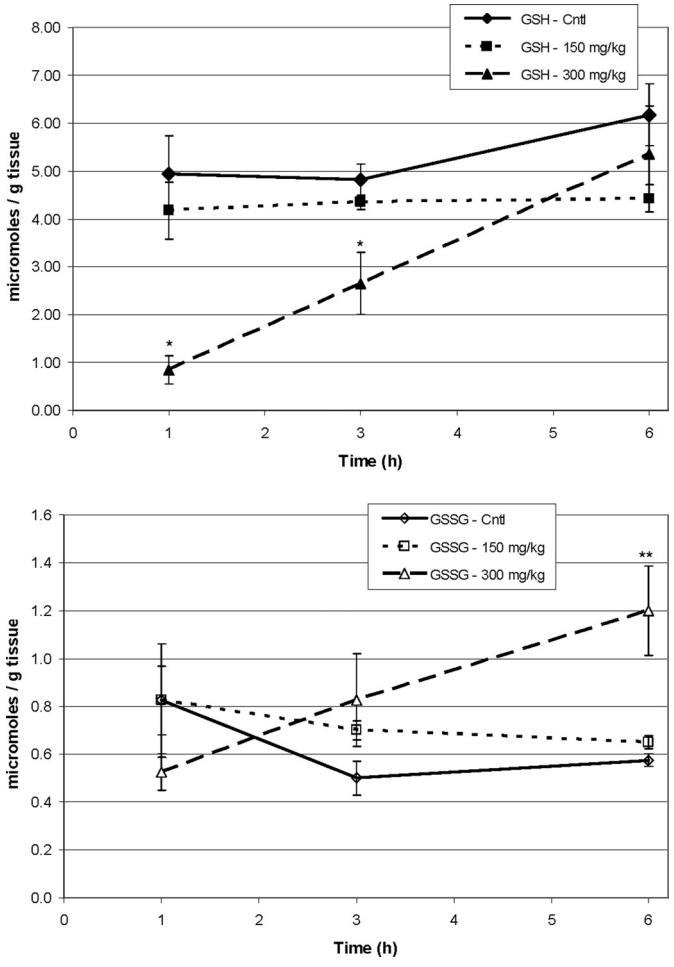

Fig. 1. Mouse hepatic GSH (top) and GSSG (bottom) levels. APAP (150 or 300 mg/kg) was administered by oral gavage, and hepatic GSH and GSSG levels were measured by Ultra Performance liquid chromatography/mass spectrometry. Top, APAP at 300 mg/kg produced a profound decrease of GSH at 1 h with recovery starting to occur within 3 h, although levels were still decreased compared with controls. *, GSH level of the 300 mg/kg group was statistically significantly decreased ($p < 0.05$) compared with the control and 150 mg/kg groups. Bottom, GSSG levels were similar to control levels at 1 and 3 h for both doses of APAP. At 6 h, APAP at 300 mg/kg produced a significant increase in GSSG levels. **, GSSG level of the 300 mg/kg group was statistically significantly increased ($p < 0.05$) compared with the control and 150 mg/kg groups. Values are mean ± S.E.M.

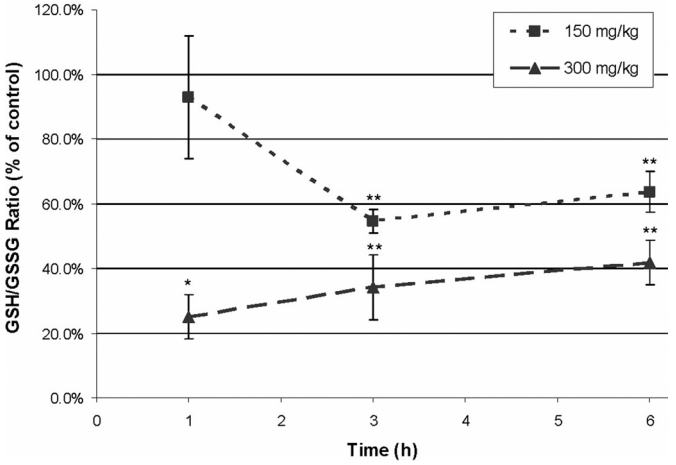

Fig. 2. Effect of APAP on mouse hepatic GSH/GSSG ratios. APAP (150 or 300 mg/kg) was administered by oral gavage, and hepatic GSH and GSSG levels were measured by Ultra Performance liquid chromatography/mass spectrometry. APAP at 300 mg/kg produced a significant decrease in the GSH/GSSG ratio at 1 h, indicative of a more oxidizing environment within the liver. The GSH/GSSG ratio increased slightly within 6 h but was still significantly decreased compared with control levels. APAP at 150 mg/kg also decreased the GSH/GSSG ratio, but the decrease was delayed and lower in magnitude compared with the 300 mg/kg group. *, GSH/GSSG ratio of 300 mg/kg group was statistically significantly decreased ($p < 0.05$) compared with the control and 150 mg/kg groups. **, GSH/GSSG of 150 and 300 mg/kg groups was statistically significantly decreased ($p < 0.05$) compared with the control group. Values are mean ± S.E.M.

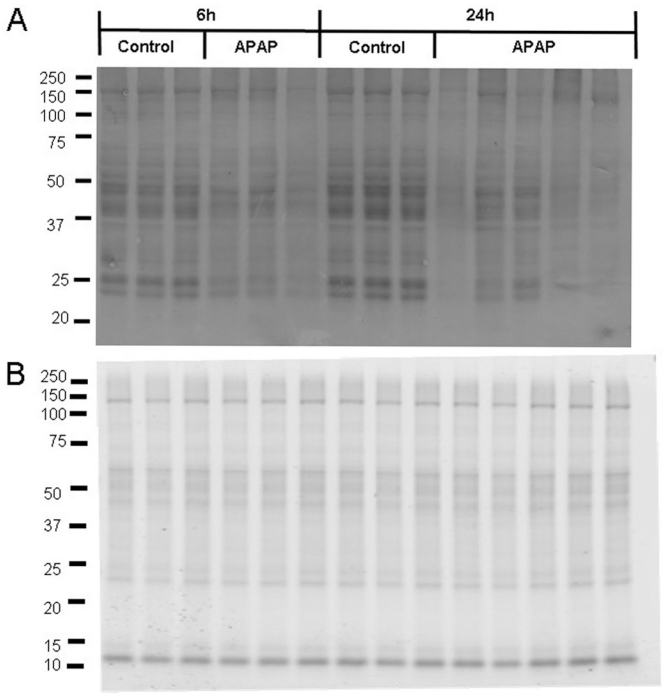

Fig. 3. The effect of APAP on protein glutathionylation in mouse liver. APAP (300 mg/kg) was administered by oral gavage, and total liver protein from 6 and 24 h was isolated and resolved on a 12% nonreducing SDS-PAGE gel. A, protein glutathionylation was determined by Western blotting using a monoclonal antibody specific for glutathionylated protein. The presented samples are representative of the other liver samples collected during the experiment and run on separate Western blots. B, the same samples were resolved on a duplicate gel followed by Coomassie staining to confirm equal loading of protein between samples.

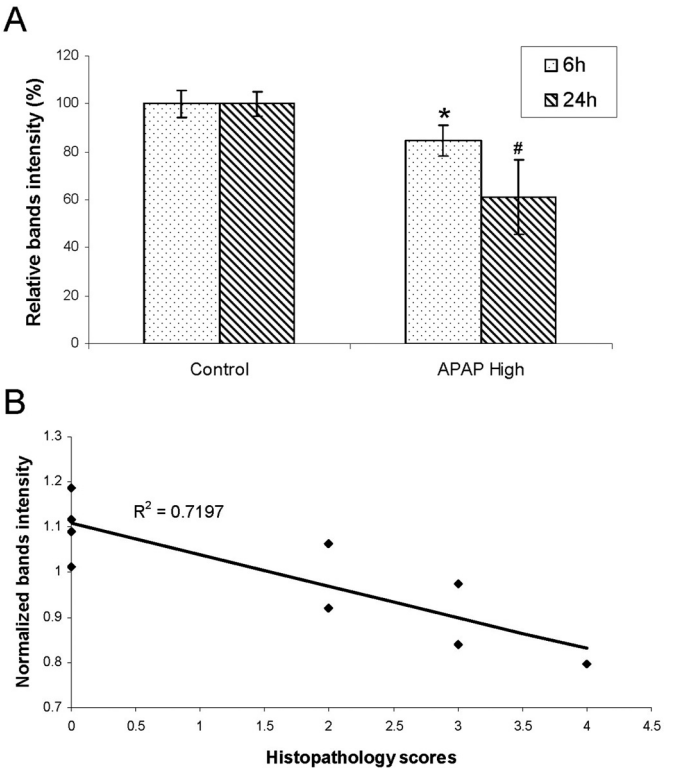

Fig. 4. Quantification of reduced protein glutathionylation in mouse liver after APAP exposure. APAP (300 mg/kg) was administered by oral gavage, and total liver protein was isolated and resolved on a 12% nonreducing SDS-PAGE gel. A, the overall glutathionylation levels were quantified by band intensity and normalized to Coomassie staining. All of the liver samples ($n \geq 4$) collected from the same time point were run on the same Western blot. Overall glutathionylation levels were reduced significantly. *, band intensity of the 300 mg/kg group was statistically significantly decreased ($p < 0.05$) compared with the control group at 6 h. #, band intensity of the 300 mg/kg group was statistically significantly decreased ($p < 0.01$) compared with the control group at 24 h. Values are mean ± S.E.M. B, correlation between the glutathionylation levels and histopathology necrosis scores at the 6-h time point. Liver necrosis was scored on a five-point scale (0, normal; 1, minimal; 2, mild; 3, moderate; 4, marked).

Lobule Zonation of APAP Adducts in Relation to Protein Glutathionylation. Western blots provided useful information on the overall changes in glutathionylation; however, they could not be used to determine the pattern of glutathionylation changes within the hepatic lobule. This is important for a compound such as APAP because it induces a specific centrilobular pattern of morphological effects and essentially spares the periportal regions. To determine whether a certain subset of cells or region of the lobule was preferentially affected, immunohistochemistry was conducted to assess the pattern of glutathionylation by using the same anti-GSH antibody used in the Western blots. In addition, the pattern of APAP adduct binding to macromolecules within the lobule was determined by using an anti-APAP antibody in serial sections. This allowed a direct comparison between the regions of the lobule that had morphological changes (hematoxylin and eosin stain), glutathionylation (anti-GSH antibody), and APAP adducts (anti-APAP antibody).

In control livers, the level of glutathionylation was uniform throughout the lobule with the exception of a layer of cells around the central veins that had high levels of glutathionylation (Fig. 5B). At 1 h after the high dose of APAP (300 mg/kg), the high level of glutathionylation seen in the controls around the central veins decreased; however, a mild increase in glutathionylation was observed throughout the central region hepatocytes (Fig. 6B). This increase in glutathionylation correlated with the region of APAP adducts (Fig. 6C). At 3 h, clear morphological changes within the centrilobular hepatocytes were observed at the high dose of APAP and decreases in glutathionylation were observed within the most inner centrilobular hepatocytes (data not shown). This pattern was accentuated at 6 h, and, in addition, a rim of hepatocytes lying on the periphery of the centrilobular region exhibited increased levels of glutathionylation (Fig. 7B). These same hepatocytes also had APAP adducts but seemed much less affected morphologically compared with the more inner centrilobular hepatocytes (Fig. 7, A and C). The low-dose APAP animals exhibited similar changes in glutathionylation; however, the changes were delayed with regard to time and were not as dramatic compared with the high dose (time-course low-dose data not shown). In contrast to the high dose of APAP, the low-dose APAP livers still exhibited the rim pattern of increased glutathionylation at 24 h (Fig. 8B). The glutathionylation within the centrilobular regions, especially for the animals that had marked centrilobular necrosis (Fig. 8C, arrowheads), was dramatically decreased relative to the other regions of the lobule (Fig. 8D). The rim pattern of increased glutathionylation was minimal at this time point in the high-dose animals but could be observed around the less affected sublobule/hepatic veins (Fig. 8D, arrows).

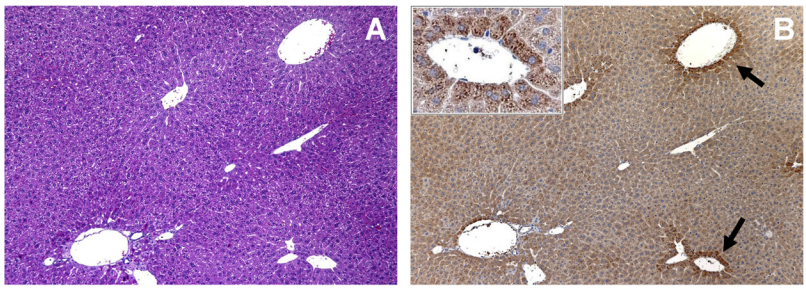

Fig. 5. Immunohistochemical detection of protein glutathionylation in vehicle control (0.5% methylcellulose) mouse liver. Two serial sections were cut to facilitate the comparison of protein glutathionylation with liver morphology. The slides were treated as follows: hematoxylin and eosin stain (A) and immunohistochemical stain using an antibody specific for glutathionylated protein (B). All immunostained slides were counterstained with hematoxylin. The layer of cells immediately surrounding the central veins exhibited strong staining for glutathionylation (B, arrows). The inset in B is a magnification of the staining around the central vein indicated by the lower arrow. Original field magnification, 100×.

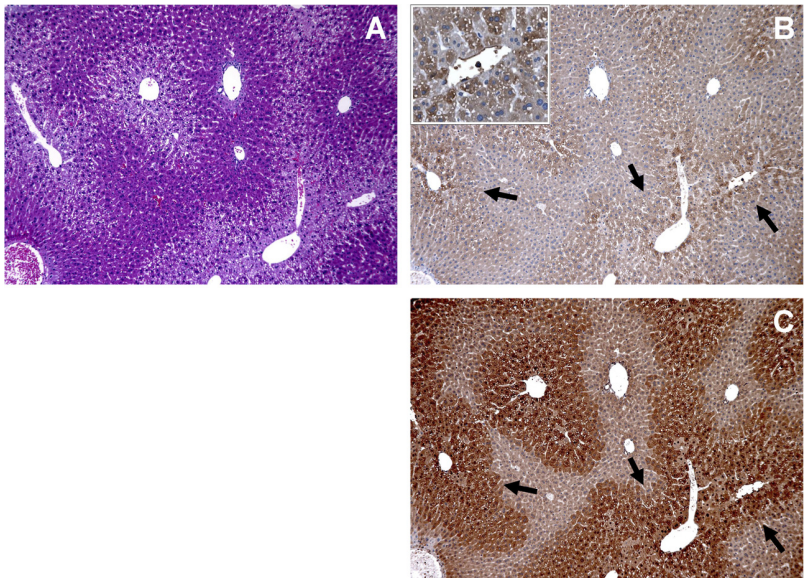

Fig. 6. Immunohistochemical detection of protein glutathionylation and APAP adduction of cellular macromolecules in mouse liver 1 h after treatment with an oral dose of 300 mg/kg APAP. Three serial sections were cut to facilitate the comparison of protein glutathionylation, APAP adduction, and liver morphology. The slides were treated as follows: hematoxylin and eosin stain (A), immunohistochemical stain using an antibody specific for glutathionylated protein (B), and immunohistochemical stain using an anti-APAP antibody (C). All immunostained slides were counterstained with hematoxylin. The centrilobular regions exhibited mild increases in glutathionylation (B, arrows) with some cells immediately around the central veins exhibiting decreased glutathionylation. The inset in B is a magnification of the staining around the central vein indicated by the lower right arrow. Areas of glutathionylation correlated with the areas of APAP adduct formation (C, arrows). Original field magnification, 100×.

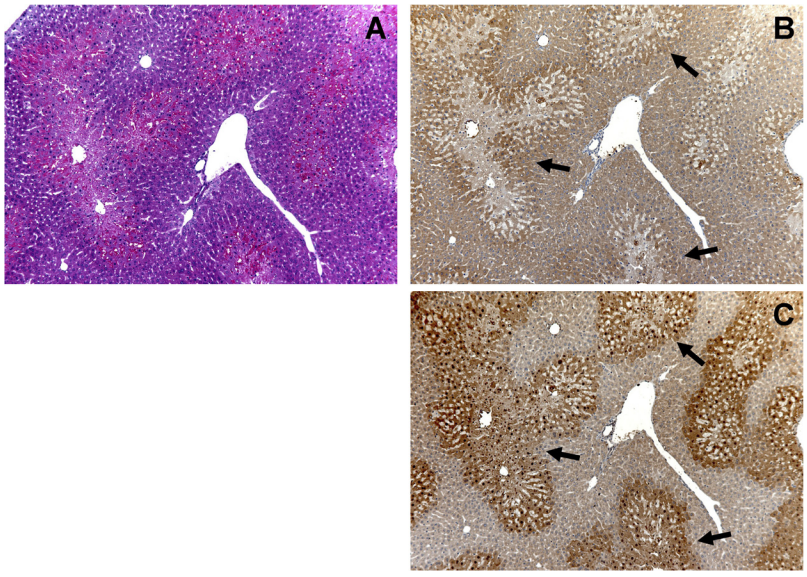

Fig. 7. Immunohistochemical detection of protein glutathionylation and APAP adduction of cellular macromolecules in mouse liver 6 h after treatment with an oral dose of 300 mg/kg APAP. Three serial sections were cut to facilitate the comparison of protein glutathionylation, APAP adduction, and liver morphology. The slides were treated as follows: hematoxylin and eosin stain (A), immunohistochemical stain using an antibody specific for glutathionylated protein (B), and immunohistochemical stain using an anti-APAP antibody (C). All immunostained slides were counterstained with hematoxylin. The cells in the periphery of the centrilobular regions exhibited increased glutathionylation (B, arrows); whereas the inner most cells of the centrilobular regions exhibited decreased glutathionylation. The region of increased glutathionylation correlated with the outermost areas of APAP adduct formation (C, arrows). Original field magnification, 100×.

Discussion

APAP overdose in mice produced classic signs of hepatotoxicity consisting of increased serum levels of ALT and AST, GSH depletion in the liver, and centrilobular necrosis. Some of these effects were manifested as early as 1 h after the dose, highlighting the rapidity of APAP-induced cellular perturbation. In line with these effects, high levels of APAP adducts to protein were observed from 1 to 6 h and were still present, albeit at lower levels, 24 h after the high dose. All of these findings are consistent with previous reports of APAP-induced hepatotoxicity via the reactive metabolite NAPQI (Roberts et al., 1991; Knight and Jaeschke, 2002; James et al., 2003).

NAPQI is believed to induce cellular injury by binding cellular macromolecules and altering their structure or function. After NAPQI binds to a sufficient number of macromolecules, or specific macromolecules, key cellular processes are altered from which the cell cannot recover. However, NAPQI

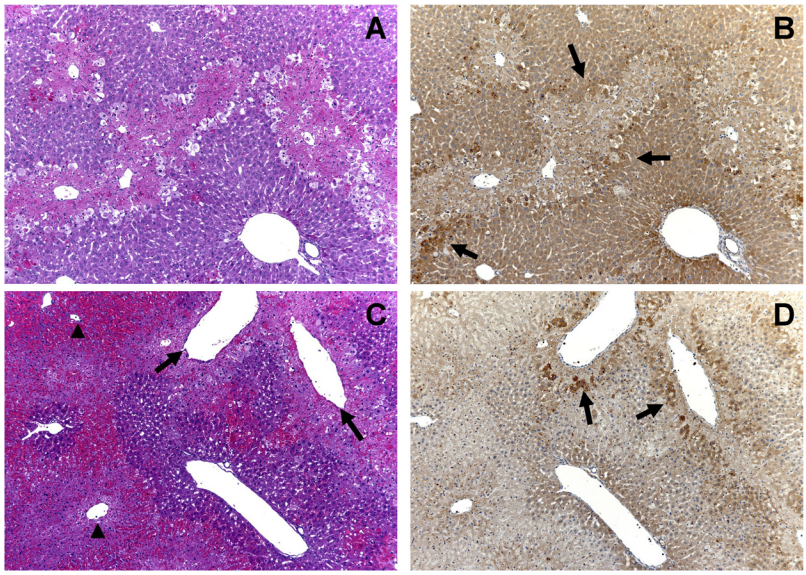

Fig. 8. Immunohistochemical detection of protein glutathionylation and APAP adduction of cellular macromolecules in mouse liver 24 h after treatment with an oral dose of 150 or 300 mg/kg APAP. Two serial sections were cut to facilitate the comparison of protein glutathionylation with liver morphology. The slides were treated as follows: hematoxylin and eosin stain (A and C) and immunohistochemical stain using an antibody specific for glutathionylated protein (B and D). All immunostained slides were counterstained with hematoxylin. At the low 150 mg/kg dose, cells at the periphery of the centrilobular lesion exhibited increased levels of glutathionylation (B, arrows). At the high 300 mg/kg dose, centrilobular necrosis was extensive (C, arrowheads), and glutathionylation was severely decreased throughout the lobule (D). Only a limited number of cells peripheral to areas of necrosis around sublobular/hepatic veins exhibited increased glutathionylation (D, arrows). Original field magnification, 100×.

also dramatically alters the redox status of hepatocytes by depleting GSH, making hepatocytes more sensitive to oxidative stress. This is reflected by the depletion of protein thiols that is observed after APAP treatment (Albano et al., 1985; Kyle et al., 1990; Tirmenstein and Nelson, 1990). Therefore, it is likely that protein structure and function are also indirectly affected by the severe depletion of GSH caused by NAPQI. This may be even more important than direct binding of NAPQI to macromolecules because the concentration of protein thiols oxidized after APAP has been shown to be more than 10-fold greater than those directly conjugated by NAPQI (Tirmenstein and Nelson, 1990).

Glutathionylation has been shown to play a regulatory role in the activity of various proteins, in a manner similar to the regulatory changes induced by protein phosphorylation (Beer et al., 2004; Chen et al., 2007; Mueller et al., 2008; Townsend et al., 2009; Bundgaard et al., 2010; Hawkins et al., 2010; Liao et al., 2010; Yang et al., 2011). Therefore, alteration of the glutathionylation status of hepatocellular proteins after hepatotoxicant insult could lead to altered function of key proteins and subsequent cellular injury. In this study, decreased global glutathionylation levels were observed as early as 1 h after the APAP dose when assessed in whole liver homogenate via Western blots. This was somewhat unexpected because the GSH, GSSG, and GSH/GSSG ratio analyses (Figs. 1 and 2) suggested that APAP induced a more oxidizing environment favoring protein glutathionylation at both the low and high doses with the effect occurring sooner and exhibiting a greater magnitude for the high dose. It is likely that other factors modulating protein glutathionylation were also changed by APAP, causing the decreased global glutathionylation. For example, the enzymes catalyzing deglutathionylation such as glutaredoxin, thioredoxin, and protein disulfide isomerase (Jung and Thomas, 1996) might be induced, which could overcompensate for the increased glutathionylation induced by the changes in GSH/GSSG. It is also possible that protein glutathionylation was differentially affected in different localizations of the liver, leading to an overall decrease of this modification (detailed below).

Although global glutathionylation was reduced, immunohistochemical analysis revealed a more complex picture. In control livers, staining was uniform throughout the lobule except for the single layer of cells immediately around the central veins that had high glutathionylation levels. One potential explanation for the high levels in this layer of cells is that oxygen tension is very low by the time the blood reaches this region of the lobule and these cells may have less capacity to deal with endogenously formed reactive species, such as reactive oxygen, possibly leading to higher levels of glutathionylation. At 1 h, glutathionylation was increased in the hepatocytes of the centrilobular region but decreased in the layer of cells immediately surrounding the central vein. The increase at 1 h was subtle but it was consistent across all treated samples and correlated with the localization of APAP binding. By 3 and 6 h, glutathionylation was increased in a rim pattern surrounding the centrilobular region but dramatically decreased elsewhere within the centrilobular region. These changes were observed for both dose groups, but the effect occurred sooner and exhibited a greater response in the high-dose group. The cells with decreased glutathionylation had clear histopathological signs of injury; whereas the ones with increased glutathionylation on the periphery had only subtle signs of injury at these time points. At 24 h, glutathionylation in the high-dose animals was dramatically decreased; whereas the low-dose animals still exhibited a rim pattern of increased glutathionylation. These time- and dose-dependent patterns of changes in protein glutathionylation are probably attributable to the differential distribution of CYP2E1 and the resulting toxicity response. Specifically, within the centrilobular area, CYP2E1 activity is high (Anundi et al., 1993), and a large amount of NAPQI is quickly produced, which causes mitochondrial dysfunctions, leading to sustained ATP shortage, GSH depletion, and eventually terminal cell death. Protein glutathionylation could not be maintained in these cells probably because 1) the proteins underwent additional irreversible oxidant damage and 2) the GSH on proteins may have been released to buffer the GSH pool. However, in the cells around the centrilobular area CYP2E1 activity is relatively low (Anundi et al., 1993), thus NAPQI production is slower, and the increased cytosolic calcium level (Tirmenstein and Nelson, 1989) could stimulate

mitochondrial oxidative phosphorylation, which helps maintain sufficient ATP levels to aid GSH biosynthesis. In addition, GSH synthesis enzymes could be induced by Nrf2 activation (Goldring et al., 2004) in these less-challenged cells after APAP exposure. Therefore, the GSH level is probably high enough to produce increased protein glutathionylation, which may help prevent the proteins from further irreversible damage or serve as a modulatory mechanism in signal transduction (Dalle-Donne et al., 2007).

The pattern of glutathionylation is consistent with indirect indicators of altered protein homeostasis. After APAP hepatotoxicity, heat shock protein 25 was shown to be induced in a similar ring pattern (Salminen et al., 1997). Heat shock proteins are known to be induced by damaged proteins and play a role in recovering damaged proteins or trafficking irreversibly damaged proteins for degradation. It is likely that altered glutathionylation disrupts protein homeostasis, such as through disulfide formation either internally or with other proteins, and the heat shock proteins try to recover these altered proteins. The ring pattern is probably caused by a threshold where some cells are too damaged to mount a recovery response; whereas others are not critically damaged and can recover from the injury by inducing protective or repair responses. It is also possible that the ring pattern of glutathionylation is an indicator of a protective response in these cells where increased glutathionylation protects the proteins from irreversible damage and helps them recover their normal state.

One likely target of altered glutathionylation after APAP injury is the mitochondria because not only does APAP affect mitochondrial function, but several key proteins, such as mitochondrial complexes I and II, have been shown to have altered function after their glutathionylation status has been changed (Beer et al., 2004; Chen et al., 2007). In addition, glutathionylation has been shown to play a role in the MPT. It was reported that carbon monoxide inhibited the MPT by glutathionylating adenine nucleotide translocase and inhibiting its pore-forming function (Queiroga et al., 2010). In the case of APAP, it is possible that decreased glutathionylation could lead to activation of the MPT through modification of pore-forming factors such as adenine nucleotide translocase. Because a large number of proteins exhibited decreased glutathionylation, it is a challenge to determine which modified proteins, if any, have an actual toxicological consequence.

In conclusion, APAP decreased protein glutathionylation in mouse liver, and even though GSH began to return to basal levels by 6 h protein glutathionylation remained depressed through 24 h. The pattern of glutathionylation within the hepatic lobule indicated that hepatocytes that are not terminally damaged may increase glutathionylation levels to either protect proteins from irreversible damage or help them recover their native state. Hepatocytes closer to the central vein with terminal damage had dramatically decreased glutathionylation levels, indicating that these cells were not able to maintain protein homeostasis. Given the dramatic decreases in hepatic GSH levels after APAP exposure, it is not surprising that protein glutathionylation also changes. Additional research will help uncover whether the alterations are simply a passive response to GSH changes or whether they are actively changed to help maintain protein homeostasis after APAP injury.

Authorship Contributions

Participated in research design: Yang, Shi, Roberts, Hinson, Beger, and Salminen.

Conducted experiments: Yang, Greenhaw, Ali, Muskhelishvili, Pence, Ando, Sun, and Davis.

Performed data analysis: Yang, Pence, and Salminen.

Wrote or contributed to the writing of the manuscript: Yang and Salminen.

References

Acharya M and Lau-Cam CA (2010) Comparison of the protective actions of *N*-acetylcysteine, hypotaurine and taurine against acetaminophen-induced hepatotoxicity in the rat. *J Biomed Sci* **17 (Suppl 1):**S35.

Adams JD Jr, Lauterburg BH, and Mitchell JR (1983) Plasma glutathione and glutathione disulfide in the rat: regulation and response to oxidative stress. *J Pharmacol Exp Ther* **227:**749–754.

Albano E, Rundgren M, Harvison PJ, Nelson SD, and Moldéus P (1985) Mechanisms of *N*-acetyl-*p*-benzoquinone imine cytotoxicity. *Mol Pharmacol* **28:**306–311.

Anundi I, Lähteenmäki T, Rundgren M, Moldeus P, and Lindros KO (1993) Zonation of acetaminophen metabolism and cytochrome P450 2E1-mediated toxicity studied in isolated periportal and perivenous hepatocytes. *Biochem Pharmacol* **45:**1251–1259.

Beer SM, Taylor ER, Brown SE, Dahm CC, Costa NJ, Runswick MJ, and Murphy MP (2004) Glutaredoxin 2 catalyzes the reversible oxidation and glutathionylation of mitochondrial membrane thiol proteins: implications for mitochondrial redox regulation and antioxidant defense. *J Biol Chem* **279:**47939–47951.

Bessems JG and Vermeulen NP (2001) Paracetamol (acetaminophen)-induced toxicity: molecular and biochemical mechanisms, analogues and protective approaches. *Crit Rev Toxicol* **31:**55–138.

Bundgaard H, Liu CC, Garcia A, Hamilton EJ, Huang Y, Chia KK, Hunyor SN, Figtree GA, and Rasmussen HH (2010) β_3 Adrenergic stimulation of the cardiac Na^+-K^+ pump by reversal of an inhibitory oxidative modification. *Circulation* **122:**2699–2708.

Burke AS, MacMillan-Crow LA, and Hinson JA (2010) Reactive nitrogen species in acetaminophen-induced mitochondrial damage and toxicity in mouse hepatocytes. *Chem Res Toxicol* **23:**1286–1292.

Chen TS, Richie JP Jr, and Lang CA (1990) Life span profiles of glutathione and acetaminophen detoxification. *Drug Metab Dispos* **18:**882–887.

Chen YR, Chen CL, Pfeiffer DR, and Zweier JL (2007) Mitochondrial complex II in the post-ischemic heart: oxidative injury and the role of protein S-glutathionylation. *J Biol Chem* **282:**32640–32654.

Dalle-Donne I, Rossi R, Giustarini D, Colombo R, and Milzani A (2007) S-glutathionylation in protein redox regulation. *Free Radic Biol Med* **43:**883–898.

Food and Drug Administration (2009) The public health problem of liver injury related to the use of acetaminophen in both over-the-counter and prescription products, at the *Joint Meeting of the Drug Safety and Risk Management Advisory Committee with the Anesthetic and Life Support Drugs Advisory Committee and the Nonprescription Drugs Advisory Committee*; 2009 June 29–30; Adelphi, MD. Food and Drug Administration, Washington, DC.

Food and Drug Administration (2011) Prescription drug products containing acetaminophen; actions to reduce liver injury from unintentional overdose. *Federal Register* **76:**2691–2697.

Goldring CE, Kitteringham NR, Elsby R, Randle LE, Clement YN, Williams DP, McMahon M, Hayes JD, Itoh K, Yamamoto M, et al. (2004) Activation of hepatic Nrf2 in vivo by acetaminophen in CD-1 mice. *Hepatology* **39:**1267–1276.

Hanawa N, Shinohara M, Saberi B, Gaarde WA, Han D, and Kaplowitz N (2008) Role of JNK translocation to mitochondria leading to inhibition of mitochondria bioenergetics in acetaminophen-induced liver injury. *J Biol Chem* **283:**13565–13577.

Hawkins BJ, Irrinki KM, Mallilankaraman K, Lien YC, Wang Y, Bhanumathy CD, Subbiah R, Ritchie MF, Soboloff J, Baba Y, et al. (2010) S-glutathionylation activates STIM1 and alters mitochondrial homeostasis. *J Cell Biol* **190:**391–405.

Hinson JA, Roberts DW, and James LP (2010) Mechanisms of acetaminophen-induced liver necrosis. *Handb Exp Pharmacol* 369–405.

Institute of Laboratory Animal Resources (1996) *Guide for the Care and Use of Laboratory Animals* 7th ed. Institute of Laboratory Animal Resources, Commission on Life Sciences, National Research Council, Washington DC.

Jaeschke H (1990) Glutathione disulfide formation and oxidant stress during acetaminophen-induced hepatotoxicity in mice in vivo: the protective effect of allopurinol. *J Pharmacol Exp Ther* **255:**935–941.

Jaeschke H (2005) Role of inflammation in the mechanism of acetaminophen-induced hepatotoxicity. *Expert Opin Drug Metab Toxicol* **1:**389–397.

James LP, McCullough SS, Lamps LW, and Hinson JA (2003) Effect of *N*-acetylcysteine on acetaminophen toxicity in mice: relationship to reactive nitrogen and cytokine formation. *Toxicol Sci* **75:**458–467.

Jung CH and Thomas JA (1996) S-glutathiolated hepatocyte proteins and insulin disulfides as substrates for reduction by glutaredoxin, thioredoxin, protein disulfide isomerase, and glutathione. *Arch Biochem Biophys* **335:**61–72.

Knight TR, Ho YS, Farhood A, and Jaeschke H (2002) Peroxynitrite is a critical mediator of acetaminophen hepatotoxicity in murine livers: protection by glutathione. *J Pharmacol Exp Ther* **303:**468–475.

Knight TR and Jaeschke H (2002) Acetaminophen-induced inhibition of Fas receptor-mediated liver cell apoptosis: mitochondrial dysfunction versus glutathione depletion. *Toxicol Appl Pharmacol* **181:**133–141.

Kyle ME, Sakaida I, Serroni A, and Farber JL (1990) Metabolism of acetaminophen by cultured rat hepatocytes. Depletion of protein thiol groups without any loss of viability. *Biochem Pharmacol* **40:**1211–1218.

Liao BC, Hsieh CW, Lin YC, and Wung BS (2010) The glutaredoxin/glutathione

system modulates NF-κB activity by glutathionylation of p65 in cinnamaldehyde-treated endothelial cells. *Toxicol Sci* **116:**151–163.
Masubuchi Y, Suda C, and Horie T (2005) Involvement of mitochondrial permeability transition in acetaminophen-induced liver injury in mice. *J Hepatol* **42:**110–116.
Matthews AM, Hinson JA, Roberts DW, and Pumford NR (1997) Comparison of covalent binding of acetaminophen and the regioisomer 3′-hydroxyacetanilide to mouse liver protein. *Toxicol Lett* **90:**77–82.
Mueller AS, Klomann SD, Wolf NM, Schneider S, Schmidt R, Spielmann J, Stangl G, Eder K, and Pallauf J (2008) Redox regulation of protein tyrosine phosphatase 1B by manipulation of dietary selenium affects the triglyceride concentration in rat liver. *J Nutr* **138:**2328–2336.
Queiroga CS, Almeida AS, Martel C, Brenner C, Alves PM, and Vieira HL (2010) Glutathionylation of adenine nucleotide translocase induced by carbon monoxide prevents mitochondrial membrane permeabilization and apoptosis. *J Biol Chem* **285:**17077–17088.
Roberts DW, Bucci TJ, Benson RW, Warbritton AR, McRae TA, Pumford NR, and Hinson JA (1991) Immunohistochemical localization and quantification of the 3-(cystein-*S*-yl)-acetaminophen protein adduct in acetaminophen hepatotoxicity. *Am J Pathol* **138:**359–371.
Salminen WF Jr, Voellmy R, and Roberts SM (1997) Differential heat shock protein induction by acetaminophen and a nonhepatotoxic regioisomer, 3′-hydroxyacetanilide, in mouse liver. *J Pharmacol Exp Ther* **282:**1533–1540.
Smith CV and Jaeschke H (1989) Effect of acetaminophen on hepatic content and biliary efflux of glutathione disulfide in mice. *Chem Biol Interact* **70:**241–248.
Srinivasan C, Williams WM, Ray MB, and Chen TS (2001) Prevention of acetaminophen-induced liver toxicity by 2(*R*,*S*)-*n*-propylthiazolidine-4(*R*)-carboxylic acid in mice. *Biochem Pharmacol* **61:**245–252.
Tirmenstein MA and Nelson SD (1989) Subcellular binding and effects on calcium homeostasis produced by acetaminophen and a nonhepatotoxic regioisomer, 3′-hydroxyacetanilide, in mouse liver. *J Biol Chem* **264:**9814–9819.
Tirmenstein MA and Nelson SD (1990) Acetaminophen-induced oxidation of protein thiols. Contribution of impaired thiol-metabolizing enzymes and the breakdown of adenine nucleotides. *J Biol Chem* **265:**3059–3065.
Townsend DM (2007) S-glutathionylation: indicator of cell stress and regulator of the unfolded protein response. *Mol Interv* **7:**313–324.
Townsend DM, Manevich Y, He L, Xiong Y, Bowers RR Jr, Hutchens S, and Tew KD (2009) Nitrosative stress-induced S-glutathionylation of protein disulfide isomerase leads to activation of the unfolded protein response. *Cancer Res* **69:**7626–7634.
Yang Y, Shi W, Chen X, Cui N, Konduru AS, Shi Y, Trower TC, Zhang S, and Jiang C (2011) Molecular basis and structural insight of vascular K_{ATP} channel gating by S-glutathionylation. *J Biol Chem* **286:**9298–9307.

Address correspondence to: William F. Salminen, Food and Drug Administration/National Center for Toxicological Research, Division of Systems Biology, 3900 NCTR Road, Jefferson, AR 72079. E-mail: william.salminen@fda.hhs.gov